

Disorder-induced Chern insulator in Harper-Hofstadter-Hatsugai model

Yoshihito Kuno

Department of Physics, Graduate School of Science, Kyoto University, Kyoto 606-8502, Japan

(Dated: May 29, 2019)

In this paper we study effects of disorder for topological Chern insulating phase in the Harper-Hofstadter-Hatsugai model. The model with half flux has bulk-band gap and thus exhibit non-trivial topological phase. We consider two typical types of disorder: random on-site disorder and Aubry-Andre type quasi-potential. By using the coupling matrix method, we clarify global topological phase diagram in terms of the Chern number. The disorders modify the gap closing nature of the system. This modification induces the Chern insulating phase even in the trivial phase parameter regime of the system in clean limit. Moreover we consider an interacting Rice-Mele model with disorder, which can be obtained from the dimensional reduction of the HHH model. Moderate strength of Disorder leads to the increase of revival event of the Chern insulator at a specific parameter point.

I. INTRODUCTION

How disorder changes topological properties of system? This issue has long been discussed and researched. Generally, nontrivial topological phase like Chern insulator (CI) is said to be robust against weak disorders since weak disorder cannot close a topological bulk-band gap of system. However, for large disorder, even if it does not break symmetry of the topological model, the topological bulk-band gap is closed. In other words, the topological phase is maintained up to large disorder. Such a topological robustness against disorder has been firstly discussed by Thouless and the colleagues [1–3]. Qualitatively, they envisaged that disorder or weak perturbation does not change a topological invariant number as long as they does not close the bulk-band gap, i.e., Chern number [4], thus the state is robust against them. But as for the robustness, quantitative level study in various concrete topological models has not been completed.

Recently, a counter intuitive phenomena has been reported in some topological models. The topological phase may be induced by disorder. For example in three dimensional topological insulator model, interesting topological phenomena induced by disorder has been theoretically suggested and numerically simulated, which is called topological Anderson insulator (TAI) [5–8]. Also in some typical two dimensional topological models, both robustness and disorder-induced topological phenomena has been reported so far [9–17]. Furthermore, very recently the Su-Schrieffer-Heeger model [18, 19] has been realized in an atomic quantum simulator [20]. The momentum space lattice in coldatoms was designed to simulated the model. There the disorder-induced topological phase characterized by the Zak phase [21] were observed. Motivated by such a recent experimental success, in this paper, we study effects of disorder for the CI phase by considering Harper-Hofstadter-Hatsugai (HHH) model [22–24] as a concrete two dimensional topological model. So far the effects of disorder in this two dimensional topological model has not been discussed and estimated yet. A complete understanding of the effects of disorder remains elusive. If we assume dimensional reduction [25], the HHH model is also important as an

ancestor model of the topological charge pumping [26], i.e., Rice-Mele (RM) model [27]. Thus, to study disorder effect of the CI phase in the HHH model is expected to give important insight to the topological charge pumping in the RM model.

This paper is organized as follows: we first show our target model in Sec. II. In Sec. III we briefly summarize a calculation method of Chern number for disordered system. In Sec. IV, we clarify disorder phase diagram and the robustness of the CI phase to disorder and the enlargement of the CI phase are studied. Then we discuss a disorder-induced CI phase by calculating the density of states (DOS) in Sec. V. Furthermore, in Sec. VI we study the RM model connected to the HHH model. In particular, we study effects of disorder for the CI phase in bosonic interacting version of the RM model. We should mention that recent experimental realization for this model [28, 29] motivates us to investigate effects of disorder for the topological phase of the model. Therefore, very recently, attention has been paid to the Bosonic RM model in some papers [30–33]. In this study, we consider out of conventional topological charge pumping trajectory. The same tendency as in the case of the non-interacting HHH model is seen. We find that event of the revival of the CI phase occurs as increasing the strength of the random potential. The results has possibility to be detectable in real experimental systems. Finally, Sec. VII is devoted to discussion and conclusion.

II. MODEL

The HHH model [22] is given by this Hamiltonian

$$H_{\text{HH}} = \sum_{m,n} \left[-t_a \hat{c}_{m+1,n}^\dagger \hat{c}_{m,n} - t_b e^{-i2\pi\beta(m-1/2)} \hat{c}_{m,n+1}^\dagger \hat{c}_{m,n} - t_c e^{i2\pi\beta m} \hat{c}_{m+1,n+1}^\dagger \hat{c}_{m,n} - t_c e^{-i2\pi\beta m} \hat{c}_{m+1,n}^\dagger \hat{c}_{m,n+1} - \Delta_0 (-1)^m n_{m,n} + \text{h.c.} \right], \quad (1)$$

where (m, n) is a lattice site on 2D square lattice and β is a flux per unit cell. $\hat{c}_{m,n}^\dagger$ ($\hat{c}_{m,n}$) is a fermionic creation (annihilation) operator.

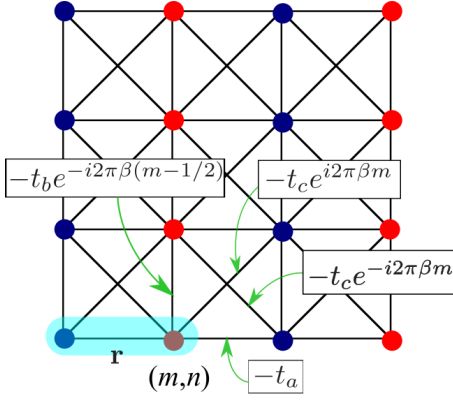


FIG. 1. Lattice structure of the HHH model. Red and blue circles represent sublattice site for half flux case ($\beta = 1/2$). The blue shaded cell is a unit cell on a position \mathbf{r} .

(annihilation) operator at site (m, n) . $n_{n,m} = c_{n,m}^\dagger c_{n,m}$ is a number operator. t_a , t_b and t_c are x – direction, y – direction and diagonal hopping amplitudes, respectively. Each hopping term is shown in Fig. 1. Δ_0 term on the last line of Eq. (1) is a staggered potential, which acts as a bulk-gap controlling term. The model belongs to AIII class in the topological classification [34, 35], i.e, it serves only chiral symmetry. For $\Delta_0 = 0$ and $t_c \neq 0$, the HHH model is known to have non-trivial topological band structure corresponding that of the Harper-Hofstadter model [22, 36]. But for $\beta = 1/2$ case with $t_c \neq 0$, the HHH model has a bulk-band gap and the band turns to be topological. If the system is in half-filling, the system exhibits the CI phase. Also, this bulk-band gap is controlled by varying the value of Δ_0 . For $\Delta_0 = 2$, the bulk-band gap is closed, then a topological phase transition occurs, the system turns into the trivial phase [23, 24]. And we consider two diagonal types of disorder: The first is on-site random potential,

$$V_d^I = \sum_{(m,n)} \frac{\mu_{m,n}}{2} n_{m,n}, \quad (2)$$

where the random potential is a uniform distributed random with the strength W_0 defined by $\mu_{m,n} \in [-W_0, W_0]$. The second is a quasi-periodic Aubry-Andre potential defined on two dimensional lattice,

$$V_d^II = \sum_{(m,n)} \frac{V_d}{2} \left[\cos(2\pi\gamma m + \phi) + \cos(2\pi\gamma n + \phi) \right] n_{m,n}, \quad (3)$$

where V_d is a potential amplitudes and γ is set on the golden ratio, $(\sqrt{5} - 1)/2$, and we introduce a phase shift parameter ϕ , which is convenient to suppress the effect boundary condition. In this study, we set $\beta = 1/2$ and $t_a = t_b = t_c = 1$ and will pay attention to half filling case.

III. CHERN NUMBER FROM A REAL SPACE HAMILTONIAN

In this paper, we estimate effects of disorder in the non-trivial topological phase in the HHH model. Disorder breaks the system translational symmetry, then the momentum representation cannot be employed. This leads to difficulty in defining and calculating the Chern number since its formula is calculated by using the system wave function represented by momentum bases [4]. However, Niu and Thouless proposed another formula of the Chern number [1, 3], which is valid even in disordered systems. They introduced twisted boundary phase parameters in a periodic boundary condition, regarded the twisted boundary phase parameters as quasi-momentum, and formulate the Chern number in terms of them. Thanks to this formulation, even though the system includes disorders, the Chern number can be defined. But so far it has been generally difficult to carry out the practical calculation for concrete lattice models in two spacial dimension. Recently, on the base of Niu and Thouless work, some papers [16, 37, 38] has suggested the real-space version of the Chern number or the Berry phase and by using it some simple disorder topological models have been studied [16, 37]. As a simplar method, the coupling-matrix method was proposed in [11] recently. In this paper, we employ the coupling-matrix method. Before proceeding any further, it is worth summerizing the coupling matrix method in detail for practical numerical calculation.

The coupling-matrix method is based on the Niu and Thouless formula [1–3]. The Chern number can be defined by two twisted boundary phase,

$$C_N = \frac{1}{2\pi i} \int_{T^2} d\theta \langle \nabla_\theta \Psi(\theta) | \times | \nabla_\theta \Psi(\theta) \rangle, \quad (4)$$

where $|\Psi(\theta)\rangle$ is a system many-body wave function, $\theta = (\theta_x, \theta_y)$ is twisted boundary phase and $\theta_x, \theta_y \in [0, 2\pi)$. These phase is introduced by twisted phase boundary condition for a single particle wave function on real space lattice $\psi(r_x, r_y)$ as $\psi(r_x + L_x, r_y) = e^{i\theta_x} \psi(r_x, r_y)$ and $\psi(r_x, r_y + L_y) = e^{i\theta_y} \psi(r_x, r_y)$ where $\mathbf{r} = (r_x, r_y)$ is a unit cell lattice site shown in Fig. 1 and $L_{x(y)}$ is a piece length of $x(y)$ -direction scaled by lattice spacing. T^2 is a torus parameter space for θ . By using the Stokes theorem for Eq. (4), C_N can be transformed into a line integral form and then let consider discretizing T^2 space $\theta \rightarrow \theta_\ell$ for later convenience of numerics. The area integral of Eq. (4) can be represented by

$$C_N = -\frac{1}{2\pi i} \prod_{\theta_\ell \in \partial T^2} \langle \Psi(\theta_\ell) | \Psi(\theta_{\ell+1}) \rangle. \quad (5)$$

∂T^2 is the boundary of the rectangular regime defined by the θ space (the area is defined by $\theta_x, \theta_y \in [0, 2\pi)$). The RHS is gauge invariant so that we need not to care the gauge dependence of the wave functions obtained in numerics [39].

Then, in considering non-interacting system the many-body wave function is given by using single particle states,

$$|\Psi(\theta_\ell)\rangle = \frac{1}{\sqrt{N_F!}} \begin{vmatrix} |\psi_{\theta_\ell}^1\rangle & \cdots & |\psi_{\theta_\ell}^{N_F}\rangle \\ \vdots & \ddots & \vdots \\ |\psi_{\theta_\ell}^1\rangle & \cdots & |\psi_{\theta_\ell}^{N_F}\rangle \end{vmatrix} \quad (6)$$

where $|\psi_{\theta_\ell}^\alpha\rangle$ is α -th single particle state with twisted phase boundary condition θ_ℓ , $\alpha = 1, \dots, N_F$. N_F is the number of maximum occupied state, determined by Fermi energy.

By using the slater determinant form of Eq. (6), $\langle\Psi(\theta_\ell)|\Psi(\theta_{\ell+1})\rangle$ in Eq. (4) is written by

$$\langle\Psi(\theta_\ell)|\Psi(\theta_{\ell+1})\rangle \equiv \det[A(\ell, \ell+1)], \quad (7)$$

where

$$A(\ell, \ell+1) = \begin{bmatrix} \langle\psi_{\theta_\ell}^1|\psi_{\theta_{\ell+1}}^1\rangle & \cdots & \langle\psi_{\theta_\ell}^1|\psi_{\theta_{\ell+1}}^{N_F}\rangle \\ \vdots & \ddots & \vdots \\ \langle\psi_{\theta_\ell}^{N_F}|\psi_{\theta_{\ell+1}}^1\rangle & \cdots & \langle\psi_{\theta_\ell}^{N_F}|\psi_{\theta_{\ell+1}}^{N_F}\rangle \end{bmatrix}. \quad (8)$$

$A(\ell, \ell+1)$ is called the coupling matrix [11].

Substituting Eq. (7) into Eq. (5), C_N is given as

$$C_N = -\frac{1}{2\pi i} \det \left[\prod_{\theta_\ell \in \partial T^2} A(\ell, \ell+1) \right]. \quad (9)$$

As a result, in order to obtain C_N , the coupling matrix $A(\ell, \ell+1)$ needs to be calculated appropriately.

It is known that the element of $A_{\ell, \ell+1}$ can be obtained well only from single particle spatial wave functions without twisted phase boundary conditions [11], i.e., $\theta = \mathbf{0}$. As in Ref.[1, 11], when one introduces the non-zero twisted boundary phase, the real space single particle wave function is given as the following Fourier transformed form,

$$\langle \mathbf{r} | \psi_\theta^\alpha \rangle = \frac{1}{\sqrt{L_x L_y}} \sum_{\mathbf{k} \in \text{BZ}} e^{-i(\mathbf{k} + \bar{\theta}) \cdot \mathbf{r}} \langle \mathbf{k} | \psi_\theta^\alpha \rangle, \quad (10)$$

where BZ represents the first Brillouin zone and $\bar{\theta} = (\theta_x/L_x, \theta_y/L_y)$. The above equation is surely satisfied with the twisted phase boundary conditions: $\psi^\alpha(r_x + L_x, r_y) = e^{i\theta_x} \psi^\alpha(r_x, r_y)$ and $\psi^\alpha(r_x, r_y + L_y) = e^{i\theta_y} \psi^\alpha(r_x, r_y)$. Here, by multiplying $e^{-i\bar{\theta}_\ell \cdot \mathbf{r}}$ on both sides of Eq. (10) with $(\theta_x, \theta_y) = \mathbf{0}$, we obtain

$$\langle \mathbf{r} | e^{-i\bar{\theta}_\ell \cdot \mathbf{r}} | \psi_{\theta=0}^\alpha \rangle = \frac{1}{\sqrt{L_x L_y}} \sum_{\mathbf{k} \in \text{BZ}} e^{-i(\mathbf{k} + \bar{\theta}_\ell) \cdot \mathbf{r}} \langle \mathbf{k} | \psi_\theta^\alpha \rangle. \quad (11)$$

Here, it is noted that the LHS in the above equation can be regarded as $\langle \mathbf{r} | \psi_{\theta_\ell}^\alpha \rangle$. Accordingly, we obtain a useful relation

$$e^{-i\bar{\theta}_\ell \cdot \mathbf{r}} | \psi_{\theta=0}^\alpha \rangle = | \psi_{\theta_\ell}^\alpha \rangle. \quad (12)$$

From this relation, once we obtain the real space wave function $|\psi_{\ell+1}^\alpha\rangle$ *without twisted boundary phases*, all wave functions with different twisted boundary phases can be constructed. Therefore, we can directly obtain the elements of coupling matrix $\langle \psi_{\theta_\ell}^\alpha | \psi_{\theta_{\ell+1}}^{\alpha'} \rangle$ from the single particle wave function without twisted boundary phase. By introducing the real space based single particle wave function as $|\psi_{\theta_\ell}^\alpha\rangle = \sum_{\mathbf{r}} c_{\mathbf{r}, \beta}^{\alpha, \theta_\ell} |\mathbf{r}, \beta\rangle$, where β is a sublattice label, $c_{\mathbf{r}, \beta}^{\alpha, \theta}$ is an expansion coefficient. The matrix element of Eq. (8) can be given as

$$\langle \psi_{\theta_\ell}^\alpha | \psi_{\theta_{\ell+1}}^{\alpha'} \rangle = \sum_{\mathbf{r}, \beta} (c_{\mathbf{r}, \beta}^{\alpha, \theta_\ell})^* e^{i(\bar{\theta}_\ell - \bar{\theta}_{\ell+1}) \cdot \mathbf{r}} c_{\mathbf{r}, \beta}^{\alpha', \mathbf{0}}. \quad (13)$$

Thus, we can obtain all elements of the coupling matrix $A(\ell, \ell+1)$ from $|\psi_{\mathbf{0}}^\alpha\rangle$. In numerics, we can easily obtain $c_{\mathbf{r}, \beta}^{\alpha, \mathbf{0}}$ by diagonalizing the real space Hamiltonian. Accordingly we can calculate each element of the coupling matrix $A(\ell, \ell+1)$ and the Chern number C_N is obtained through Eq. (9).

In the coupling matrix method, as long as we obtain the real space single particle wave function even in a system without translational invariance, we can obtain the C_N through Eq. (9).

IV. DISORDER PHASE DIAGRAM OF THE HHH MODEL

In this section, we calculate the global topological phase diagrams for the two disorder potentials V_d^I and V_d^{II} . We take periodic boundary condition in the system. In particular, we focus that how the disorder potentials modify the phase boundary between trivial ($C_N = 0$) and non-trivial topological CI phase ($C_N = 1$) in the HHH model. These phases are identified by the Chern number C_N . By using the coupling matrix method introduced in the previous section, we determined the ground-state phase diagram. Figure. 2 (a) is the result of V_d^I disorder case. The system size is $(L_x, L_y) = (20, 20)$. This result indicates that the CI phase is robust up to $W_0 \sim 11$ for small Δ_0 regime and we find that for moderate disorder strength the regime of the CI phase characterized by $C_N \sim 1$ is enlarged due to the random on-site potential, the phase boundary is clearly beyond the phase boundary in the clean limit case $\Delta_0 = 2$ as shown as the red line in 2 (a). In this phase diagram, when we increase W_0 from zero at a certain value of Δ_0 , a little larger than $\Delta_0 = 2$, the system exhibits a interesting transition flow: trivial phase \rightarrow CI phase \rightarrow trivial phase. Figure. 3(a) shows the detailed behavior of C_N for typical fixed Δ_0 's. We capture a clear plateau with $C_N = 1$ for $\Delta_0 = 2.1$. This is a disorder-induced CI phase by on-site random disorder, i.e., the revival of the CI phase. For larger Δ_0 the plateau is getting to decrease as shown in Fig. 3(a). Similar transition flow, so far, has been reported in some other topological models except for the HHH model [9, 12, 14, 15, 17, 20].

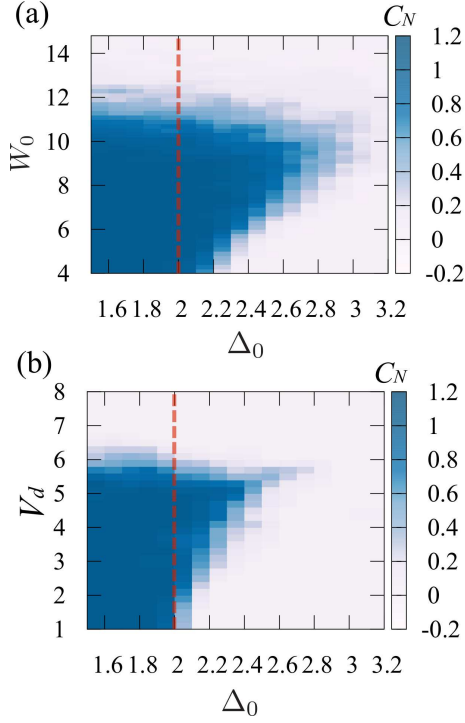


FIG. 2. (a) Random on-site potential case. We averaged over 40 random on-site samples. (b) Quasi-periodic potential case. We averaged over 40 samples with different values of ϕ . The red lines represent the conventional topological phase transition line in the clean limit, $\Delta_0 = 2$.

Next, we consider the quasi periodic Aubry-Andre potential case V_d^{II} . Here, in order to suppress the boundary effect coming from the fact that the quasi-periodic potential is discontinuous on the boundary, we average over ϕ , where ϕ is divided into 40 parts between 0 and 2π . The result is shown in Fig. 2 (b). The unit cell lattice size is $(L_x, L_y) = (20, 20)$. As same with the on-site random disorder case V_d^{I} , the CI phase is robust against the quasi-periodic disorder up to $V_d \sim 6$ in $\Delta_0 < 2$ and interestingly we find that even in the quasi-periodic disorder, the regime of the CI phase is enlarged beyond $\Delta_0 > 2$ in moderate values of V_d . Therefore, the HHH model exhibits the disorder-induced CI phase, which is defined in $\Delta_0 > 2$ regime, for both on-site random and quasi-periodic potential.

In addition we calculate the bulk-band gap near the phase boundary between the CI phase and trivial phase in moderate values of V_d in V_d^{II} with $\phi = 0$. Here, the bulk-band gap E_{gap} is defined by the energy difference between $(L_x L_y / 2)$ -th and $(L_x L_y / 2 + 1)$ -th eigenenergy in the real-space Hamiltonian of the HHH model. We plot the distribution of the bulk-band gap E_{gap} in Fig. 3 (b). The result indicates that E_{gap} in the disorder-induced CI regime has small but finite value, the transition from the disorder-induced CI to trivial phase seems to be originated from the conventional gap closing nature in typical topological phase transition: gapfull \rightarrow gapless critical

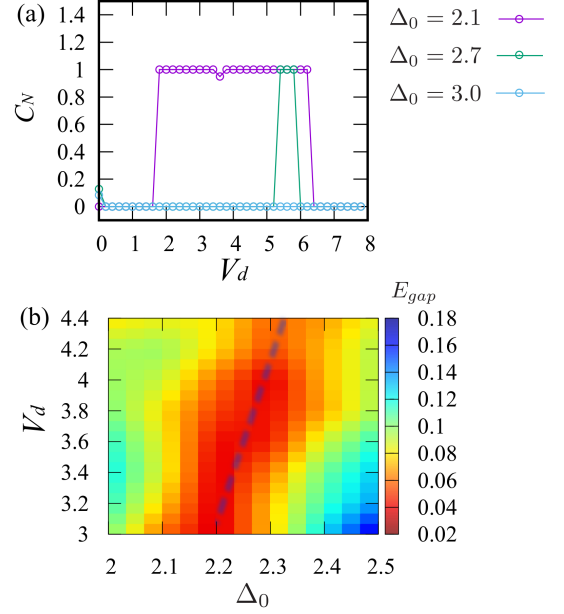


FIG. 3. (a) Disorder dependence of C_N for $\Delta_0 = 2.1$ 2.7 and 3. (b) Bulk-band gap distribution near the phase boundary between the disorder-induced CI phase and trivial phase. The blue dashed line is an approximate phase boundary where the value of the bulk-band gap is much small.

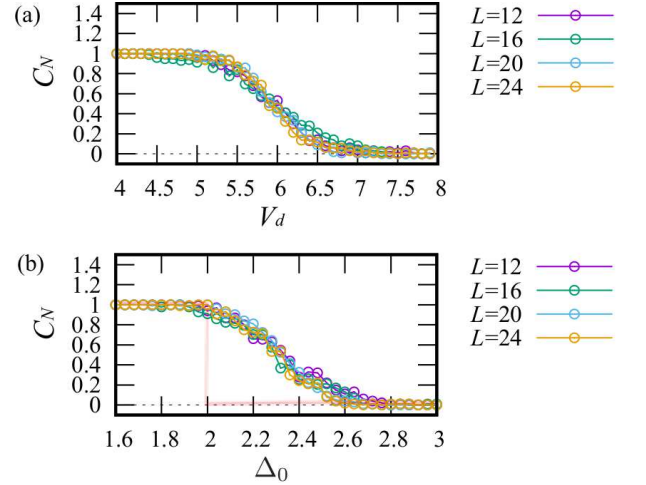


FIG. 4. (a) System size dependence of C_N for $\Delta_0 = 1.6$. (b) System size dependence of C_N for $V_d = 4$. The light red line represents the conventional CI phase transition point in clean limit, $\Delta_0 = 2$. Here, $L_x = L_y = L$. For all data, we averaged over 40 samples with different values of ϕ .

point \rightarrow gapfull as varying a parameter. For more detail, we also calculate the DOS in the next section.

To consolidate the global phase diagrams in Fig. 2, we estimate the system size dependence of the coupling matrix method. We focus on the V_d^{II} disorder case. Figure 3 (a) and (b) shows the system size dependence of the C_N both from the conventional CI phase to trivial phase and from the disorder-induced CI phase to trivial phase. For

both cases, the results indicates weak system size dependence. Therefore, our calculation results are expected to much close to those of thermodynamic limit.

V. DENSITY OF STATE

To strength the existence of the disorder-induced CI, the gap closing property should be studied in detail. The density of states (DOS) [40] gives a signal to close the bulk-band gap and also localization properties. The DOS is defined as follows:

$$\rho(E_i) = \frac{1}{N_D} \sum_k \delta(E_i - E_k). \quad (14)$$

Here, E_i and N_D are i -th energy eigenvalue and the Hilbert space dimension, respectively. Practically, we calculate $\rho(E_i)$ by setting an small but finite energy window ΔE , in which E_i is centered.

Here we consider the quasi-periodic potential V_d^{II} of Eq. (3) with $\phi = 0$ and calculate the DOS around the band center ($E_i \sim 0$) at typical parameter points in the phase diagram of Fig. 2(b). Figure 5 is the result of the DOS for $(L_x, L_y) = (62, 124)$ system size. The data are at $(\Delta_0, V_d) = (2.1, 4)$, $(2.1, 8)$ and $(1, 4)$, corresponding to the disorder-induced CI phase, the trivial phase and the conventional CI phase, respectively. For the conventional CI point $(\Delta_0, V_d) = (2.1, 4)$, the values of $\rho(E_i)$ around $E_i = 0$ clearly is zero. This means that the conventional CI has clear large bulk-band gap. For the trivial phase point $(\Delta_0, V_d) = (2.1, 8)$, the values of $\rho(E_i)$ is finite even around $E_i = 0$. This indicates in large disorder regime, the trivial phase has no bulk-band gap, the system tends to have metallic properties. For the disorder-induced CI point $(\Delta_0, V_d) = (2.1, 4)$, the values of $\rho(E_i)$ slightly around $E_i = 0$ is zero. That is, this result indicates that the bulk-band gap has survived slightly. By combining this result and the direct bulk-band gap calculation in Fig. 5 (b), we conclude that the disorder remains the bulk-band gap open even through the parameter Δ_0 exceeds the value of the CI phase transition point in clean limit. We expect that this mechanism about the emergence of the disorder-induced CI is somewhat different from that of the TAI [5, 6, 8]. The TAI is believed to occur from a mobility gap [8, 18] and there the bulk-band gap is vanished, then the values of $\rho(E_i)$ is finite even around $E_i = 0$ [8].

Also, before closing this section, we should comment that the data at $(\Delta_0, V_d) = (2.1, 4)$ exhibits sharp peaks at $E_i \sim \pm 1$. This is a signal for the existence of the mobility edge. Similar behavior so far has been reported in other model [12]. Therefore, in the disorder-induced CI phase the system spectrum includes also weak localization properties. This result is reminiscent of the result in Ref.[16].

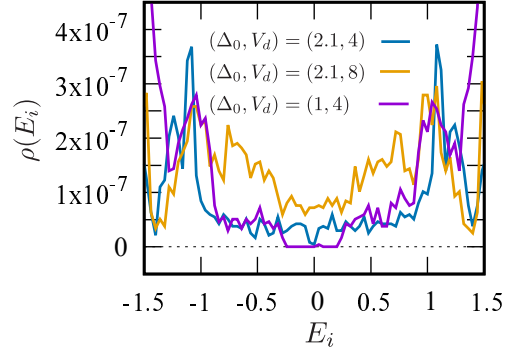


FIG. 5. Density of states. The blue-, yellow- and purple-line data are at the disorder-induced CI phase $(\Delta_0, V_d) = (2.1, 4)$, the trivial phase $(\Delta_0, V_d) = (2.1, 8)$ and the conventional CI phase $(\Delta_0, V_d) = (1, 4)$, respectively.

VI. POSSIBILITY FOR DISORDER-INDUCED CI IN A ONE-DIMENSIONAL REDUCED MODEL

For the previous sections, we has focused on the non-interacting HHH model and found the disorder-induced CI phase. In this section, we study whether such a phase also exists in an interacting topological system. Generally, it is difficult to numerical-simulate the two dimensional HHH model with interaction. Thus, we consider a one-dimensional (1D) model obtained by considering a dimensional reduction of the HHH model. The 1D model can be derived by using the dimensional reduction technique [25]. A two-dimensional model H_{2D} is reduced to a one-dimensional model with adiabatic parameter $H_{1D}(\rho)$,

$$H_{2D} = \int \frac{d\rho}{2\pi} H_{1D}(\rho). \quad (15)$$

where ρ is an adiabatic parameter. We apply the above formula to the HHH model of Eq. (1), then assume bosonic system with an on-site interaction and add an on-site random potential. The 1D model is given by

$$H_{1D}(\rho) = \sum_m \left[-J_m(\rho)(b_{m+1}^\dagger b_m + \text{h.c.}) + (\Delta_m(\rho) + W_m)b_m^\dagger b_m + \frac{U}{2}b_m^\dagger b_m(b_m^\dagger b_m - 1) \right]. \quad (16)$$

This is a bosonic interacting Rice-Mele (RM) model, m is 1D lattice site, b_m^\dagger (b_m) is a bosonic creation (annihilation) operator at site m , U is on-site interaction, W_i is uniform distributed random potential with the strength W_0 defined by $W_m \in [-W_0/2, W_0/2]$. Also the parameters $J_m(\rho)$ and $\Delta_m(\rho)$ are given by

$$J_m(\rho) = t_a + 2t_c(-1)^m \cos(\rho), \quad (17)$$

$$\Delta_m(\rho) = [2t_b \sin(\rho) - \Delta_0](-1)^{m+1}. \quad (18)$$

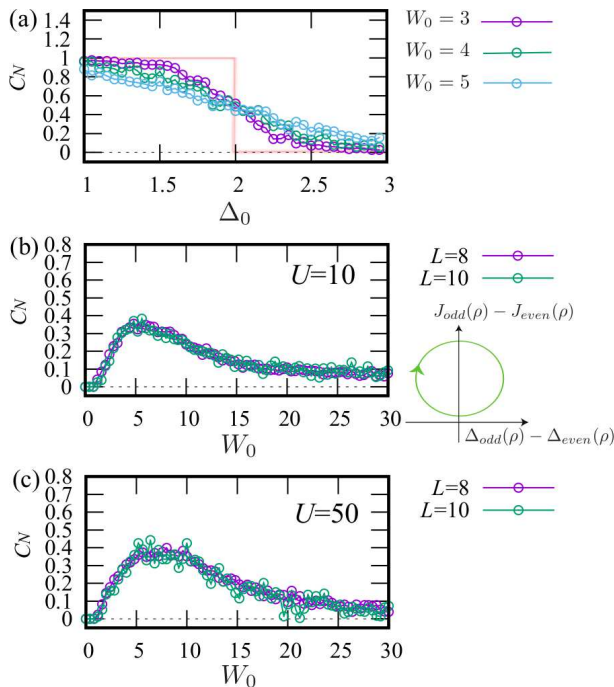


FIG. 6. Disorder dependence of C_N . (a) The case for the non-interacting HHH model with x -site dependent on-site random potential. The light red line represents the conventional CI phase transition in the clean limit, $\Delta_0 = 2$. The case for 1D interacting RM model with $U = 10$ (b) and $U = 50$ (c). For both cases, the particle density is $1/2$ and we averaged over 400 and 1000 disorder samples for $L = 8$ and $L = 10$.

The y -direction hopping and on-site staggered potential in the HHH model are transformed into a modulated on-site potential in the 1D model and the NNN hopping into a modulated part of the hopping in the 1D model. The bosonic RM model has already been realized in cold-atom experiments [28, 29]. Δ_0 -term in Eq. (18) can be implemented as an additional staggered lattice potential in the real experimental systems. In the real experiments, the Chern number C_N in the RM model can be extracted as the shift of the Wigner center in optical lattice.

In order to detect the disorder-induced CI phase as shown in the previous sections, we consider half-filled system (boson particle density $1/2$) and periodic boundary condition, and employ the exact diagonalization [41–43]. To judge topological phase, we used the Chern number [44] parameterized by ρ and twisted boundary phase α [45, 46].

To begin with, for comparison, we calculate the fermionic HHH model of Eq. (1) with only x -site dependent on-site random potential, written by $\sum_{(m,n)} W_m c_{(m,n)}^\dagger c_{(m,n)}$. By using the dimensional reduction of Eq. (15), the model can be also mapped into the non-interacting RM model with on-site disorder in one spacial dimension. Figure 6 (a) is Δ_0 -dependence of the Chern number for typical moderate disorder strength. Here, the topological phase transition becomes somewhat

crossover-like centered on the clean limit transition point $\Delta_0 = 2$. Even in $\Delta_0 > 2$, the averaged value of C_N is finite to some extent, that is, this indicates that the CI characterized by $C_N = 1$ often is generated depending on disorder samples. Let us turn to the exact diagonalization results for the interacting bosonic RM model as shown in Fig. 6 (b) and (c). Here, we set $\Delta_0 = 2.1$ and vary the disorder strength W_0 . For both interaction strength $U = 10$ and 50 , the data exhibits a fairly large values (~ 0.4) of the average of C_N in a moderate disorder strength regime and the behavior seems independent of the system size and the interaction strength U . We expect that the proliferation tendency of the value of C_N in a moderate disorder strength regime is a signal for the disorder-induced CI state. As same with the non-interacting fermion case in Fig. 6 (a), even the interacting bosonic RM model also exhibits revival event of the CI state.

VII. DISCUSSION AND CONCLUSION

In this paper, we studied effect of disorder for the CI in the Harper-Hofstadter-Hatsugai model. Two kind of the disorder term were assumed: on-site random and quasi-periodic Aubry-Andre potential. The global phase diagram were calculated by using the coupling matrix method. We found that in the HHH model a disorder-induced CI phase is appeared for both type of disorder. We calculated the bulk-band gap and the DOS. From these calculation, the disorder-induced CI has small but finite bulk-gap. This situation is somewhat different from topological Anderson insulator, where the origin is mobility gap. Furthermore, we detected the disorder-induced CI phase for an interacting bosonic RM model connected to the HHH model by using the dimensional reduction. There, we found similar results in the non-interacting fermionic HHH model, that is, even interacting bosonic RM model exhibits revival event of the CI state induced by random potential disorder in the level of the exact diagonalization calculation. This revival event may be tested in real experimental cold atom system [28, 29] since bosonic atom experiments reach much low temperature regime, which can avoid finite temperature effects. And random potential can be implemented by using a speckle laser [47, 48]. Also for the interacting bosonic RM model, numerically, a larger system size maybe accessible with greater computational resources. It would be an interesting problem for future work.

All finding in this study may appear in the topological Haldane model, which has been realized in coldatom experiments [49, 50]. For the system, it may be interesting how the disorder-induced CI phase appears. And as a future prospect, effects of disorder may be tractable by the replica theory [51]. There, random on-site disorder potential can be transformed into an effective interaction term made of different replica fields. This interaction term may renormalize a mass term (corresponding to Δ_0

term in the HHH model), as a result, it may lead the phase boundary shift of topological phase transition, i.e., generates the disorder-induced CI phase.

ACKNOWLEDGMENTS

Y. K. thank Y. Takahashi and S. Nakajima for helpful discussion. Y. K. acknowledges the support of a Grant-in-Aid for JSPS Fellows (No.17J00486).

-
- [1] Q. Niu and D. J. Thouless, J. Phys. A: Math. Gen. **17** 2453-2462 (1984).
 - [2] Q. Niu and D. J. Thouless, J. Phys. A. **17**, 2453 (1984).
 - [3] Q. Niu, D. J. Thouless, and Y-S. Wu, Phys. Rev. B **31**, 3372 (1985).
 - [4] D. J. Thouless, M. Kohmoto, M. P. Nightingale, and M. den Nijs, Phys. Rev. Lett. **49**, 405 (1982).
 - [5] H. M. Guo, G. Rosenberg, G. Refael, and M. Franz, Phys. Rev. Lett. **105**, 216601 (2010).
 - [6] C. W. Groth, M. Wimmer, A. R. Akhmerov, J. Tworzydło, and C. W. J. Beenakker, Phys. Rev. Lett. **103**, 196805 (2009).
 - [7] J. Li, R. L. Chu, J. K. Jain, and S. Q. Shen, Phys. Rev. Lett. **102**, 136806 (2009).
 - [8] Y. Y. Zhang, R. L. Chu, F. C. Zhang, and S. Q. Shen, Phys. Rev. B **85** 035107 (2012).
 - [9] T. Liu and H. Guo, Phys. Lett. A **382**, 3287 (2018).
 - [10] J. Qin and H. Guo, Phys. Lett. A **380**, 2317 (2016).
 - [11] Y. F. Zhang, Y. Y. Yang, Y. Ju, L. Sheng, D. N. Sheng, R. Shen, and D. Y. Xing, Chin. Phys. B **22**, 117312 (2013).
 - [12] E. V. Castro, M. P. Lopez-Sancho, and M. A. H. Vozmediano, Phys. Rev. B **92**, 085410 (2015).
 - [13] K. -I. Imura, Y. Yoshimura, T. Fukui, Y. Hatsugai, arXiv:1706.04493 (2017).
 - [14] A. Yamakage, K. Nomura, K. I. Imura, and Y. Kuramoto, J. Phys. Soc. Japan **80**, 053703(2011).
 - [15] P. V. Sriluckshmy, K. Saha, and R. Moessner, Phys. Rev. B **97**, 024204 (2018).
 - [16] E. Prodan, T. L. Hughes, and B. A. Bernevig, Phys. Rev. Lett. **105**, 115501 (2010).
 - [17] I. Mondragon-Shem, T. L. Hughes, J. Song, and E. Prodan, Phys. Rev. Lett. **113**, 046802 (2014).
 - [18] S.-Q. Shen, Topological Insulators (Springer-Verlag, Berlin, 2012).
 - [19] J. K. Asboth, L. Oroszlány, and A. Pályi, A Short Course on Topological Insulators (Springer International Publishing, New York, 2016), Vol. 919.
 - [20] E. J. Meier, F. A. An, A. Dauphin, M. Maffei, P. Massignán, T. L. Hughes, and B. Gadway, Science **362**, 929 (2018).
 - [21] J. Zak, Phys. Rev. Lett. **62**, 2747 (1989).
 - [22] Y. Hatsugai, and M. Kohmoto, Phys. Rev. B **42**, 8282 (1990).
 - [23] J.-H. Zheng, T. Qin, and W. Hofstetter, Phys. Rev. B **99**, 125138 (2019).
 - [24] B. Irsigler, J.-H. Zheng, and W. Hofstetter, arXiv: 1904.03091 (2019).
 - [25] Y. E. Kraus and O. Zilberberg, Phys. Rev. Lett. **109**, 116404 (2012).
 - [26] D. J. Thouless, Phys. Rev. B **27**, 6083 (1983).
 - [27] M. J. Rice and E. J. Mele, Phys. Rev. Lett. **49** 1455 (1982).
 - [28] M. Lohse, C. Schweizer, O. Zilberberg, M. Aidelsburger, and I. Bloch, Nat. Phys. **12**, 350 (2016).
 - [29] S. Nakajima, T. Tomita, S. Taie, T. Ichinose, H. Ozawa, L. Wang, M. Troyer, and Y. Takahashi, Nat. Phys. **12**, 296 (2016).
 - [30] Y. Qian, M. Gong, and C. Zhang, Phys. Rev. A **84**, 13608 (2011).
 - [31] R. Li and M. Fleischhauer, Phys. Rev. B **96**, 085444 (2017).
 - [32] Y. Ke, X. Qin, Y. S. Kivshar, and C. Lee, Phys. Rev. A **95**, 063630 (2017).
 - [33] A. Hayward, C. Schweizer, M. Lohse, M. Aidelsburger, and F. Heidrich-Meisner, Phys. Rev. B **98**, 245148 (2018).
 - [34] A. P. Schnyder, S. Ryu, A. Furusaki, and A. W. W. Ludwig, Phys. Rev. B **78**, 195125 (2008).
 - [35] A. Kitaev, in Advances in Theoretical Physics: Landau Memorial Conference, edited by V. Lebedev and M. Feiguelfman, AIP Conf. Proc. No. 1134 (AIP, Melville, NY, 2009), p. 22.
 - [36] D. R. Hofstadter, Phys. Rev. B **14**, 2239 (1976).
 - [37] R. Bianco and R. Resta, Phys. Rev. B **84**, 241106(R) (2011).
 - [38] R. Resta, Eur. Phys. J. B **79**, 121 (2011)
 - [39] B. A. Bernevig. *Topological Insulators and Topological Superconductors*. Princeton University Press, 2013.
 - [40] A. Weise, G. Wellein, A. Alvermann, and H. Fehske, Rev. Mod. Phys. **78**, 275 (2006).
 - [41] P. Prelovsek and J. Bonca, Strongly Correlated Systems: Numerical Methods (Springer, Berlin, 2013), Vol. 176.
 - [42] M. Zhang and R. X. Dong, Eur. J. Phys. **31** 591 (2010).
 - [43] D. Raventos, T. Gras, M. Lewenstein and B. Julia-Diaz, J. Phys. B **50** 113001 (2017).
 - [44] T. Fukui, Y. Hatsugai and H. Suzuki, J. Phys. Soc. Japan **74** 1674 (2005).
 - [45] S. L. Zhu, Z. D. Wang, Y. H. Chan, and L. M. Duan, Phys. Rev. Lett. **110**, 075303 (2013).
 - [46] Y. Kuno, K. Shimizu and I. Ichinose, New J. Phys. **19** 123025 (2017).
 - [47] T. Schulte, S. Drenkelforth, J. Kruse, W. Ertmer, J. Arlt, K. Sacha, J. Zakrzewski, and M. Lewenstein, Phys. Rev. Lett. **95**, 170411 (2005).
 - [48] D. Clement, A. F. Varon, J. A. Retter, L. Sanchez-Palencia, A. Aspect, and P. Bouyer, New J. Phys. **8**, 165 (2006).
 - [49] G. Jotzu, M. Messer, R. Desbuquois, M. Lebrat, T. Uehlinger, D. Greif, and T. Esslinger, Nature (London) **515**, 237 (2014).
 - [50] L. Asteria, D. T. Tran, T. Ozawa, M. Tarnowski, B. S. Rem, N. Flaschner, K. Sengstock, N. Goldman, C. Weitenberg, Nat. Phys. Advanced Online Publication (2019)
 - [51] S. F. Edwards and P. W. Anderson: J. Phys. F **5**, 965 (1975).